Thermal oxidation of $Si_{1-x-y}Ge_xC_y$ epitaxial layers characterized by Raman and infrared spectroscopies

A. Cuadras,[a] B. Garrido, and J. R. Morante
Department of Electronics, University of Barcelona, Marti i Franques 1, 08028 Barcelona, Spain

C. E. Hunt
Department of Electrical and Computer Engineering, University of California, Davis, One Shields Avenue, Davis, California 95616

McD Robinson
Lawrence Semiconductor Research Laboratory, 2300 West Huntington Drive, Tempe, Arizona 85282

(Received 15 April 2004; accepted 11 October 2004; published 28 December 2004)

Thermal dry oxidation of $Si_{1-x-y}Ge_xC_y$ epilayers, over a wide range of compositions ($0<x<0.6$ and $0<y<0.05$), is studied to assess the feasibility of its integration into silicon processes. It is found that differing oxidation conditions, with different x and y values, result in measurably different final amounts of Ge segregation and stress in the resultant oxides. Raman and infrared spectroscopies have been used to characterize the influence of oxidation conditions on the oxide and on the epilayer properties. It is found that a linear relationship exists between Raman shifts and C concentration in the epilayer. It is also found that the Raman band related to Si–Si bonds splits into two peaks. This double-peak structure is attributed to the development of a region closest to the oxide/epilayer interfaces which is enriched with Ge due to its rejection from the oxidation front. It is concluded that oxidation temperatures lower than 900 °C will more readily avoid this segregation, whereas oxidations at higher temperatures, for shorter times, are better suited to minimize the effects of strain generated during the processing. © *2005 American Vacuum Society.* [DOI: 10.1116/1.1829061]

I. INTRODUCTION

$Si_{1-x}Ge_x$ is considered a potential alternative to improve the performance of microelectronics silicon technology. $Si_{1-x}Ge_x$-based commercial heterojunction bipolar transistors (HBT) can effectively improve some figures of merit over those of standard silicon devices. Nevertheless, $Si_{1-x}Ge_x$ has some inherent inconveniences like critical thickness limitations and boron outdiffusion, and it is also rather unsuitable for process integration. To achieve further improvements in the field of group IV epilayers, it has been proposed to introduce carbon in $Si_{1-x}Ge_x$. $Si_{1-x-y}Ge_xC_y$ minimizes the strain in the epilayer, resulting in increased critical thickness[1] and also show reduced boron outdiffusion.[2,3] The theoretical study of HBTs based on $Si_{1-x-y}Ge_xC_y$ also demonstrates further improvements over the figures of merit achieved for $Si_{1-x}Ge_x$.[4] This has already been demonstrated experimentally by Meyerson.[5]

The complete integration of $Si_{1-x-y}Ge_xC_y$ in CMOS (complementary metal-oxide-semiconductor) technologies has not been possible yet. The main inhibition is the metastability of the epitaxial layers when subjected to the standard high-temperature processing sequence of CMOS. On the one hand, the low solubility of carbon in silicon makes epitaxial growth difficult, as carbon tends to occupy both substitutional and interstitial positions. On the other hand, the CMOS processes involve high temperature processing so that epilayer stability is also compromised. Furthermore, studies of thermal oxidation of $Si_{1-x}Ge_x$ indicate a segregation of Ge from the oxidation front[6–8] a large density of interface states.[9,10] In this work, we study the benefits of including carbon in $Si_{1-x}Ge_x$ epilayers on thermal oxidation at temperatures above 900 °C. It is expected that the tensile strain induced by substitutional carbon (interstitial carbon does not contribute to strain) compensates the compressive strain induced by Ge so that the effects of thermal processing can be minimized.

Raman spectroscopy has proven useful in measuring mechanical strain in silicon-based devices and has also been used in the characterization of as-grown $Si_{1-x-y}Ge_xC_y$ epilayers. There is fairly good correlation between the Raman and the measured strain in $Si_{1-x}Ge_x$. They are empirically described[11,12]

$$\kappa_{\mathrm{Si-Si}}(x) = 520\ \mathrm{cm}^{-1} - 68x - 830\varepsilon_{II}(x), \tag{1}$$

$$\kappa_{\mathrm{Si-Ge}}(x) = 400.5\ \mathrm{cm}^{-1} - 14.2x - 575\varepsilon_{II}(x), \tag{2}$$

$$\kappa_{\mathrm{Ge-Ge}}(x) = 282.5\ \mathrm{cm}^{-1} - 16x - 384\varepsilon_{II}(x), \tag{3}$$

where κ is the Raman shift in cm^{-1}, x is the Ge fraction of $Si_{1-x}Ge_x$, and

$$\varepsilon_{\parallel}(x) = \frac{a_{\parallel} - a_{\mathrm{Si}_{1-x}\mathrm{Ge}_x}}{a_{\mathrm{Si}_{1-x}\mathrm{Ge}_x}} \tag{4}$$

is the mismatch between the epilayer and the substrate ($a_{\parallel}$ and $a_{\mathrm{Si}_{1-x}\mathrm{Ge}_x}$ are the parallel lattice and the unstrained $Si_{1-x}Ge_x$ lattice parameters). The first terms in Eqs. (1)–(3)

[a]Present address: Dept. Electronic Engineering, EPSC-UPC Av. Canal Olimpic s/n 08860, Castelldefels, Spain; electronic mail: cuadras@eel.upc.es

TABLE I. Percentage of Ge and C content in sample sets and thicknesses of the epilayers. Samples in Sets 460 and 452 are strained and samples in set 432 are relaxed.

	X	Y	d_{layer} (nm)
452L	0.21	0.0	101.3
452N	0.22	0.015	127.2
452M	0.22	0.02	121.7
452I	0.19	0.025	96.6
452O	0.22	0.03	125.9
460C	0.11	0.0006	243.3
460E	0.10	0.001	243.1
460G	0.10	0.022	232.7
460I	0.11	0.008	202.3
432W	0.47	0.01	144.9
432X	0.45	0.02	158.6
432Y	0.43	0.03	148.9
432Z	0.5–0.6	0.04–0.05	144.9

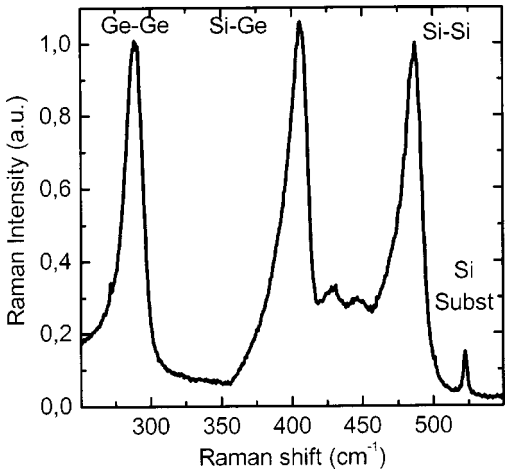

FIG. 1. Raman spectrum for $Si_{1-x-y}Ge_xC_y$, for a relaxed sample with $x=0.43$ and $y=0.03$. Three main bands are resolved: the Ge–Ge band, at 290 cm^{-1}, the Si–Ge band at 406 cm^{-1}, the strained Si–Si band at 500 cm^{-1}. The bulk Si–Si band at 520 cm^{-1} is used as reference.

are the vibrational frequencies of the different modes. The second terms show the linear dependence of the lattice strain with Ge concentration and were found using data fitting. The third terms in Eqs. (1)–(3) are the result of the strain between the epitaxial layer and the substrate. The effects of strain in $Si_{1-x-y}Ge_xC_y$ due to carbon concentration have also been studied and are found to vary linearly with substitutional carbon content. Rücker and Methfensel propose an additional term for the Si-Si band: $y\cdot 210$ cm^{-1}.[13]

Expressions (1)–(3) confirm a linear relationship between composition and epitaxial strain for both germanium and carbon, because of Vegard's law. The presence of Ge in unstrained epilayers shifts Si–Si bonds toward lower frequencies, while carbon has the opposite effect. The shift toward higher frequencies indicates increasing compressive strain in the layer whereas decreasing frequency correlates to decreasing compressive strain, or the onset of tensile strain. Using Raman spectroscopy we can measure the evolution of strain during the oxidation process as a function of the initial epilayer composition.

To separate the effects of thermal processing on the layer considered up to now from the effects on the oxide, we use Fourier transform infrared (FTIR) spectroscopy to evaluate the oxide, as Raman cannot measure these amorphous layers well enough. The FTIR vibrational modes of the oxide bonds are well defined and characterized.[14,15] Their shifts may depend on different parameters, as oxide thickness, image charge effects, film inhomogeniety, and oxide stress.[16] We focus here on the dependence of the asymmetric stretching (mode TO_3) as a function of oxide stress.

II. EXPERIMENT

Samples with compositions from $x=0.1$-0.6 of Ge and $y=6\times10^{-4}-0.05$ of C were studied. The compositions and thicknesses of the as-grown epilayers were measured by Rutherford backscattering spectroscopy (RBS) and x-ray diffraction (XRD). Results are described in Table I. Epitaxy was accomplished by atmospheric pressure chemical vapor deposition.[17] Layer thicknesses were around 100–200 nm. Absolute Ge and C concentration were determined by RBS and crystalline quality was verified by channeling for the as-grown $Si_{1-x-y}Ge_xC_y$ layers. Additional x-ray diffraction confirmed the crystallinity and the degree of strain of the samples. From RBS and XRD, we notice that not all Ge and C were substitutionally incorporated in the samples, as part of them remain interstitial.

Prior to oxidation, samples were cleaned in a H_2SO_4: H_2O_2 bath followed by a dip in diluted HF and rinsed in deionized water. Following the cleaning, samples were kept in an N_2 atmosphere until undergoing dry oxidation. We have straightforwardly extended this cleaning procedure from silicon to $Si_{1-x-y}Ge_xC_y$ with satisfactory results elsewhere.[18] Rapid thermal oxidation between 900–1000 °C was performed, as well as conventional dry oxidation at 900 °C for 35 min. Oxide thicknesses were around 15–25 nm.

Raman spectroscopy measurements were performed in backscattering geometry using a Jobin Yvon T64000 spectrometer fitted with a metalographic microscope. An argon laser with a 488 nm blue line was used for excitation at room temperature. FTIR spectra were measured with a BOMEM DA8 spectrometer, with a glowar infrared source, a KBr beamsplitter, and a Mercury-Cadmium-Tellurium (MCT) detector. The effective detection window ranged from 400 to 4000 cm^{-1}. Absorption spectra were monitored in normal incidence in order to characterize the oxide, structurally. Non-oxidized samples were used as references.

III. RESULTS AND DISCUSSIONS

A. As-grown layers

We first analyze by Raman spectroscopy the crystallinity and the degree of strain of the epitaxial growth of the layers presented in Table I. We find that $x<0.2$ samples are completely strained, whereas for higher concentrations of Ge ($x=0.4$) the layers are relaxed. In Fig. 1 we present a typical

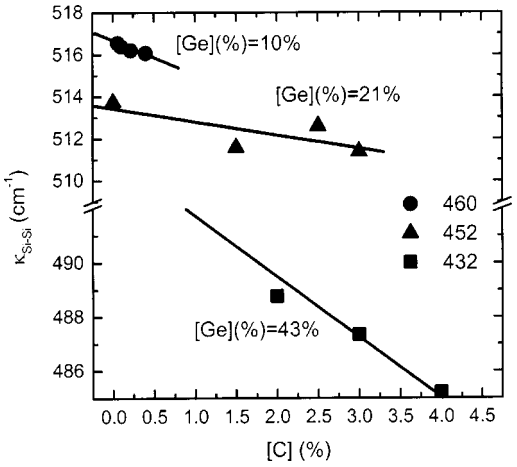

FIG. 2. Linear dependence of the Si–Si Raman shifts with carbon concentration for $Si_{1-x-y}Ge_xC_y$ samples. Note the large shift between samples with $x<25\%$ and samples with $x>40\%$ due to strain relief. All three sets show a linear trend with carbon concentration.

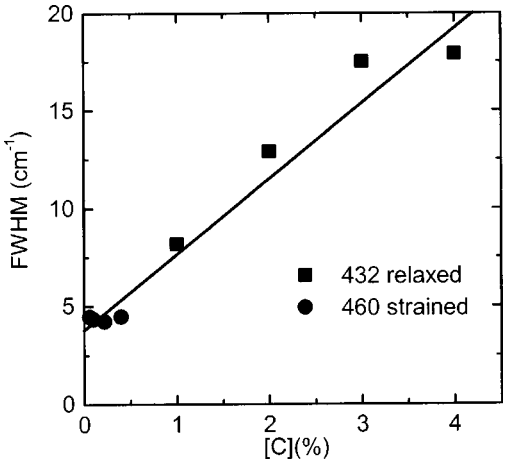

FIG. 3. FWHM dependence of the Raman Si–Si peak on carbon concentration. The relationship is approximately linear (correlation factor $r=0.96$), so that peaks widen with larger carbon concentrations.

$Si_{0.54}Ge_{0.43}C_{0.03}$ spectrum. There are four Raman peaks clearly resolved. The one located at around 298 cm^{-1} corresponds to the Ge–Ge vibrational mode. This peak is strongly dependent on Ge concentration but for concentrations below $x=0.1$ is poorly resolved. The peak centered at 415 cm^{-1} corresponds to the Si–Ge bond. There are two bands related to the Si–Si bond. The first corresponds to the unstrained bulk Si–Si bond, which is centered at 520 cm^{-1} and that we have taken as a reference in assessing peak shifts. The second one corresponds to the compressively strained Si in the epilayer and is shifted toward a lower frequency with respect to the 520 cm^{-1} band. The two smaller peaks centered at 428 and 447 cm^{-1} have been attributed to the Si–Ge ordering in the layer.[19]

We study now the shifts in the different bands as a function of the carbon composition of the layers. The resulting Si–Si shifts for different $Si_{1-x-y}Ge_xC_y$ samples are depicted in Fig. 2. From this graph we point out two different behaviors. First, we notice a linear dependence with carbon concentration. Second, we observe a significant difference in the magnitude of shifts corresponding to strained (samples with $x<0.25$) as opposed to unstrained layers, samples with $x=0.4$. We discuss them separately, starting with the latter. X-ray diffraction measurements confirmed that $Si_{0.6-y}Ge_{0.4}C_y$ is fully relaxed ($\varepsilon_{\parallel}=0$) while $Si_{0.9-y}Ge_{0.1}C_y$ and $Si_{0.8-y}Ge_{0.2}C_y$ are fully strained. Thus, the shift of the peak for the samples with $x=0.4$ is due to the high Ge concentration ($x=0.4$) since the strain has been completely relieved, in agreement with Eq. (1). On the other hand, according to expression (1), the shifts found for the samples with lower Ge concentration ($x=0.1,0.2$) are a combination of both the effects of x and of the mismatch strain.

With respect to the peak shifts with C concentration, it varies inversely linearly for $y<0.04$. We fit the experimental data with a linear regression to find a slope $\Delta\kappa/y$ of (-129 ± 30) cm^{-1} for the strained set (460) and (-220 ± 30) cm^{-1} for the relaxed set (432). Clearly, the carbon-induced shifts in the strained set (460) have a smaller magnitude than in the relaxed set (432). As a consequence, we infer a strong dependence of carbon on the epitaxial strain in the layer. In the literature, these shifts have already been explained by the presence of carbon in the lattice confining the phonons.[13]

The full width at half maximum (FWHM) of the Si–Si strained peak is also sensitive to carbon concentration, as is evident in Fig. 3 where a clear increase of the width of the peak corresponds to increasing y values. We suggest that this behavior is due to the lattice disorder induced by a random distribution of carbon, when the concentration exceeds 0.5%.

B. The layer after the oxidation

We now analyze the effects of thermal oxidations on $Si_{0.8}Ge_{0.2}C_y$ samples, with the objective of further understanding layer degradation and segregation of Ge into the Si. We have performed oxidations at 1000 °C up to 20 min and at 900 °C for 35 min. In all cases we have assured that the oxide thickness is never more than one tenth of the as-grown epitaxial layer thickness. A typical set of spectra for $Si_{0.8}Ge_{0.2}C_{0.015}$ is presented in Fig. 4, with the Ge–Ge, Si–Ge, and Si–Si bands, as described in the Introduction, clearly resolved.

The positions and the shapes of the three peaks change with the oxidation process. The most dramatic change is in the Si–Si peak, which splits into two peaks. In Fig. 5 we have subtracted the unstrained Si–Si reference band at 520 cm^{-1} in order to better appreciate the structure of the strained peak. We believe that the explanation for the Si–Si peak splitting is the segregation of Ge into the Si substrate, which we have already characterized by means of a study of the concentration as a function of depth from the oxidation front, and reported previously.[18,20] This segregation forms an enriched Ge layer just below the oxidation front, giving rise to a multilayer structure. This multilayer is responsible for the splitting of the strained peak because a different Ge con-

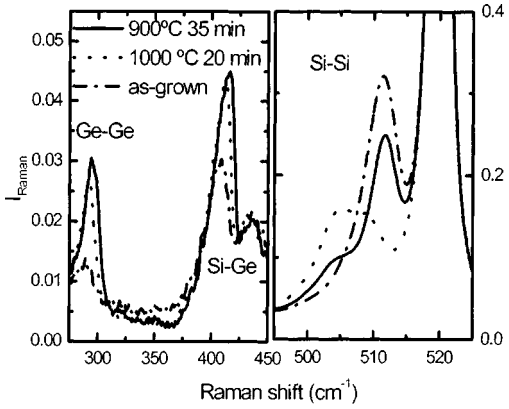

FIG. 4. Raman spectra of oxidized $Si_{1-x-y}Ge_xC_y$ samples. The comparison of the different oxidation conditions show a splitting of the Si–Si strained peak for oxidation at 1000 °C, while the Si–Ge and Ge–Ge peaks show a larger intensity for oxidation at 900 °C (35 min).

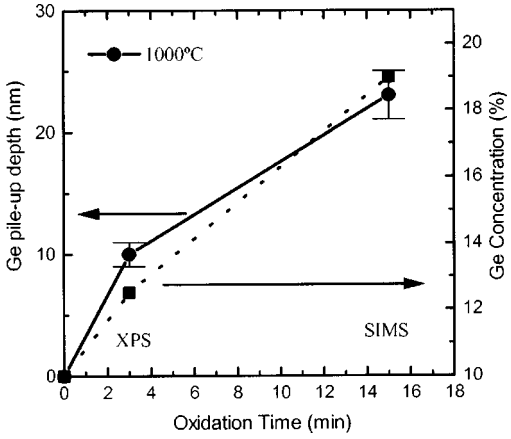

FIG. 6. On the left axis, Ge penetration depth in the epilayer from the oxidation front. On the right axis, Ge accumulation in the oxidation front as a function of oxdidation time at 1000 °C. Ge accumulation increases with time, along with the depth penetration.

centration in each layer leads to a different peak shift. To quantify the Ge accumulation in this enriched layer we can rewrite Eq. (1)

$$k_{\mathrm{Si-Si}}(x) = 520\ \mathrm{cm}^{-1} - 68x + 210y - 830\varepsilon_{\parallel}(x), \tag{5}$$

where we have also included the term related to carbon following Rücker and Methfensel.[21] We have demonstrated elsewhere that carbon leaves substitutional position when oxidized in these conditions (1000 °C or 35 min at 900 °C).[22] Thus, this term will only contribute in as-grown samples. If we compare the Raman shifts of Fig. 5 for each peak, we can estimate the Ge segregation. The strained Si–Si peak remains in the 510 cm^{-1} while the splitted peak shifts toward 505–506 cm^{-1}. This peak is due to strained Si–Si bond in a Ge richer region. Substituting these values in expression (5) we obtain that Ge concentration increases up to 26%. These results agree fairly well with Ge accumulation obtained after concentration depth profiles (shown in Fig. 6) for $Si_{0.9-y}Ge_{0.1}C_y$ samples where we observe an accumulation of 15% for 10 min at 1000 °C, although further measurements to establish a definitive correlation will be required.

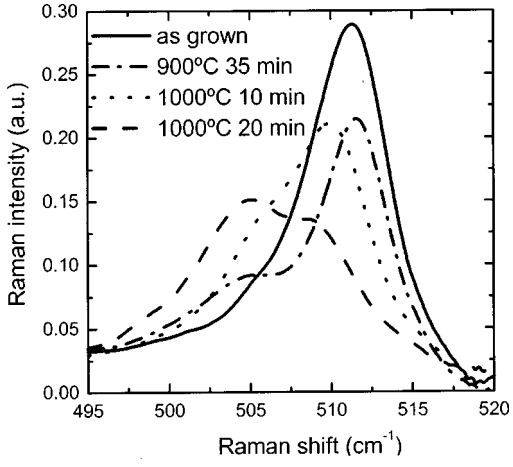

FIG. 5. Strained Si–Si Raman peak for $Si_{0.8}Ge_{0.2}C_{0.0015}$. We have removed the Si bulk peak (centered at 520 cm^{-1}) for a better definition of the strained Si–Si peak splitting. This splitting is due to the segregation of Ge at the interface.

In samples with $x=0.2$ it is also possible to study the Si–Ge and the Ge–Ge bands. In Fig. 4, we observe that the Ge–Ge and Si–Ge bands are strongly asymmetric; their intensity increases with oxidation time while their FWHM decreases. In Fig. 6 we have plotted the shifts of the Si–Ge band as a function of oxidation time for samples with two different carbon concentrations. We observe how the shift toward higher frequencies increases with oxidation time. We attribute these correlations (intensity, FWHM, and shifts) to the multilayer formation as explained in the previous paragraph. The enrichment of Ge leads to a positive shift in agreement with Eqs. (2) and (3), and moreover, a larger Ge concentration leads to a signal enhancement.

We also observe that while the Si–Si peak shows a stronger dependence on the oxidation at 1000 °C, the Si–Ge and Ge–Ge peaks are more sensitive to the longer oxidations at 900 °C, as is observed from the peak positions in Figs. 4 and 7. This can also be explained in terms of the Ge accumulation below the oxidation front. The Ge distribution depends on the oxidation conditions.[18,20] At lower temperatures ($<$950 °C) and longer oxidation times, Ge can diffuse deeper into the epilayer so that the Ge segregation shows a low concentration increase in a deeper depth. For oxidation at higher temperature ($>$1000 °C) for shorter times, Ge is accumulated just below the oxidation front, increasing the Ge concentration without diffusing into the epilayer. The Raman measurement is more sensitive to the long-range diffusion in the case of the Si–Ge and Ge–Ge bands while for the case of the Si–Si band, it is more sensitive to increasing Ge accumulation in a thinner layer at the oxidation front.

C. Oxides grown from different epilayers

As we have mentioned in the Introduction, vibrational frequencies depend on different parameters, like oxide thickness, image charge effects, inhomogeneities in the film, and

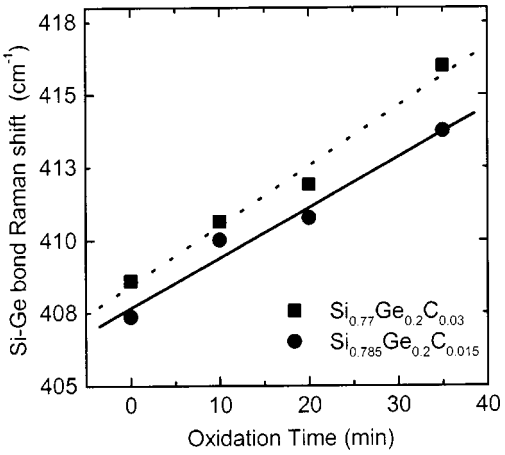

FIG. 7. Si–Ge Raman peak shifts for $Si_{1-x-y}Ge_{0.2}C_y$ after different oxidations. A linear dependence is found, with oxidation time. The different carbon concentration introduces an offset between the two fittings. The Ge–Ge peak shifts similarly. Oxidations for 10 and 20 min have been performed at 1000 °C while oxidation for 35 min have been performed at 900 °C.

compressive stress. Oxide thicknesses are of the order of 25 nm for all samples. Thus, vibrational frequencies will not depend on oxide thickness or image charge effects.[23] Furthermore, as we have already reported strong dependences of oxide kinetics on stress,[24] we now justify the FTIR shifts on the basis of oxide stress as a function of the epilayer composition.

We study the growth of the oxide on $Si_{1-x-y}Ge_xC_y$ with fixed $x=0.2$ and different carbon concentrations, along with a silicon reference sample free of stress. The results show slight, but significant, differences in peak positions and shapes, depending on the sample concentration and the thermal cycle undertaken. To carry out an accurate comparison between the different samples we have studied the shifts in the position of the vibrational mode TO_3 with respect to pure SiO_2. It is currently accepted that shifts toward larger frequencies are related to more relaxed oxides.[11,12] In Fig. 8(a), we plot the absorbance of the TO_3 modes in oxides grown in different epilayers, We find a shift toward larger frequency, as seen in Fig. 8(b). This is an expected trend since thicker oxides relax through viscous flow.[25,26] An unexpected observation is that the oxides grown in the alloy layers are more relaxed than those grown on bulk silicon, irrespective of thickness. We believe that this result agrees with the relative magnitude of strain in $Si_{1-x-y}Ge_xC_y$. For these measurements, the Ge concentration is the same for all the samples ($x=0.2$) whereas y is varied. Carbon compensates the compressive strain induced by Ge in the epilayer. We thus find that oxides grow more relaxed in epilayers with a compressive strain.[19]

From Fig. 8(b) we also observe that oxides grown at 1000 °C are more relaxed than those grown at 900 °C for a longer time, regardless of the carbon concentration. These results are already reported for silicon and are justified by means of the viscous flow relaxation model.[19,26]

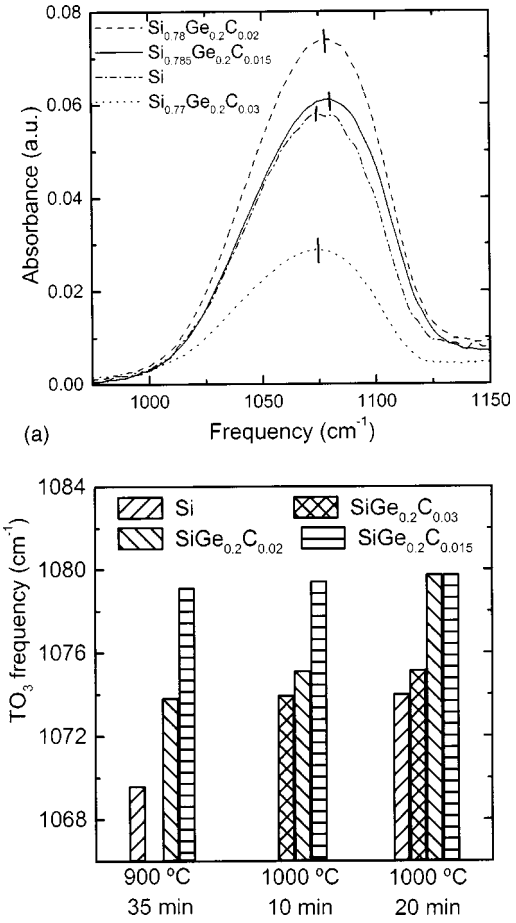

FIG. 8. (a) FTIR absorbance spectra for the TO_3 mode of oxides grown onto different $Si_{1-x-y}Ge_xC_y$ epilayers, showing a shift with y toward lower frequency. (b) TO_3 mode shifts for samples with $x=0.2$ and varying carbon concentration. Samples oxidized at 1000 °C show the largest shifts, i.e., the oxides are more relaxed.

IV. CONCLUSIONS

We have studied the influence of carbon on the vibrational bands of $Si_{1-x-y}Ge_xC_y$ with different x and y. We have found that the peak shifts follow a linear relationship with substitutional C concentration. We have characterized the effects of high temperature oxidation on $Si_{1-x-y}Ge_xC_y$ epilayers. We have found that the Raman Si–Si band associated with strained Si in the epitaxial layer splits into two peaks during oxidation at 1000 °C. We have attributed this effect to the accumulation of Ge in a layer below the oxidation front. As a consequence, the Si–Si bond gets more strained due to the local increase of Ge. Thus, as the goal is to preserve the $Si_{1-x-y}Ge_xC_y$ epilayer during the thermal process and to avoid Ge segregation, oxidation at a lower temperature (900 °C) for a longer time are more convenient. We have also demonstrated that with more carbon in the epilayer, the grown oxide is more relaxed. We have concluded that the strain generated during the oxidation, due to the mismatch between the oxide and the epilayer, is better accommodated in processes at high temperatures for short times.

In conclusion, the complexity of strained $Si_{1-x-y}Ge_xC_y$ epilayer oxidation requires certain tradeoffs in the oxidation

conditions, as the more relaxed oxides are obtained at the highest temperatures (1000 °C), whereas the preservation of epilayer uniformity requires lower temperatures (900 °C).

[1]J. W. Matthews, J. Vac. Sci. Technol. **12**, 126 (1975).
[2]H. Rücker and B. Heinemann, Solid-State Electron. **44**, 783 (2000).
[3]M. Franz, K. Pressel, and P. Gaworzewski, J. Appl. Phys. **84**, 709 (1998).
[4]A. Biswas and P. K. Basu, Solid-State Electron. **45**, 1885 (2001).
[5]B. S. Meyerson, IBM J. Res. Dev. **44**, 391 (2000).
[6]J. Xiang, N. Herbots, H. Jacobsson, P. Ye, S. Hearne, and S. Whaley, J. Appl. Phys. **80**, 1857 (1996).
[7]A. Cuadras, B. Garrido, C. Bonafos, R. Morante, L. Fonseca, and K. Pressel, Microelectron. Reliab. **40**, 829 (2000).
[8]B. Garrido, A. Cuadras, C. Bonafos, J. R. Morante, L. Fonseca, M. Franz, and K. Pressel, Microelectron. Eng. **48**, 207 (1999).
[9]D. K. Nayak, J. S. Park, J. S. C. Woo, K. L. Wang, and I. C. Ivanov, J. Appl. Phys. **76**, 982 (1994).
[10]D. K. Nayak, K. Kamjoo, J. S. Park, J. C. S. Woo, and K. L. Wang, IEEE Trans. Electron Devices **39**, 56 (1992).
[11]M. I. Alonso and K. Winer, Phys. Rev. B **39**, 10056 (1989).
[12]J. C. Tsang, P. M. Mooney, F. Dacol, and J. O. Chu, J. Appl. Phys. **75**, 8098 (1994).
[13]H. Rücker and M. Methfensel, Phys. Rev. B **52**, 11059 (1995).
[14]G. Lucovsky, J. Non-Cryst. Solids **227–230**, 1 (1998).
[15]B. Garrido, Ph.D Thesis, University of Barcelona, 1993.
[16]K. T. Quenney, M. K. Weldon, J. P. Chang, Y. J. Chabal, A. B. Gurevich, J. Sapjeta, and R. L. Opila, J. Appl. Phys. **87**, 1322 (2000).
[17]McD. Robinson, C. E. Hunt, Z. Atzmon, and L. Ling, U. S. Patent No. 6,064,081 (filed 1999).
[18]A. Cuadras, B. Garrido, C. Bonafos, R. Morante, L. Fonseca, and K. Pressel, Microelectron. Reliab. **40**, 829 (2000).
[19]D. J. Lockwood, K. Rajan, E. W. Fenton, J. M. Baribeau, and M. W. Denhoff, Solid State Commun. **61**, 465 (1987).
[20]B. Garrido, A. Cuadras, C. Bonafos, J. R. Morante, L. Fonseca, M. Franz, and K. Pressel, Microelectron. Eng. **48**, 207 (1999).
[21]H. Rücker and M. Methfensel, Phys. Rev. B **52**, 11059 (1995).
[22]A. Cuadras, B. Garrido, C. Bonafos, R. Morante, L. Fonseca, and K. Pressel, Microelectron. Reliab. **40**, 829 (2000).
[23]C. Martinet and R. A. B. Devine, J. Appl. Phys. **77**, 4343 (1995).
[24]B. Garrido, A. Cuadras, C. Bonafos, J. R. Morante, L. Fonseca, M. Franz, and K. Pressel, Microelectron. Eng. **48**, 207 (1999).
[25]E. A. Irene, E. Tierney, and J. Angilello, J. Electrochem. Soc. **129**, 2594 (1982).
[26]G. Charitat and A. Martinez, J. Appl. Phys. **55**, 909 (1984).